Nano Energy 97 (2022) 107199

Contents lists available at ScienceDirect

Nano Energy

journal homepage: www.elsevier.com/locate/nanoen

Transparent self-powered triboelectric sensor based on PVA/PA hydrogel for promoting human-machine interaction in nursing and patient safety☆

Jin Yang [a,b,1], Jie An [b,c,1], Yanshuo Sun [a,b], Jianjun Zhang [a,b], Lulu Zu [b,c], Hao Li [a,b], Tao Jiang [a,b,c,*], Baodong Chen [b,c,d,*,2], Zhong Lin Wang [b,c,e]

[a] School of Chemistry and Chemical Engineering, Guangxi University, Nanning, Guangxi 530004, PR China
[b] Beijing Institute of Nanoenergy and Nanosystems, Chinese Academy of Sciences, Beijing 101400, PR China
[c] School of Nanoscience and Technology, University of Chinese Academy of Sciences, Beijing 100049, PR China
[d] Institute of Applied Nanotechnology, Jiaxing, Zhejiang 314031, PR China
[e] School of Materials Science and Engineering Georgia Institute of Technology, Atlanta, GA 30332-0245, USA

ARTICLE INFO

Keywords:
Triboelectric sensor
Self-powered
PVA/PA hydrogel
Human-machine interaction
Medical nursing

ABSTRACT

Human-machine interaction (HMI) has made great progress in the intelligent medical system, realizing the interaction between patients, medical staff and medical equipment. Here, we report a triboelectric nanogenerator with the flexible-stretchable polyvinyl alcohol/phytic acid (PVA/PA) hydrogel for self-powered HMI sensing in intelligent medical system. Benefiting from effective optimization design of materials, it possesses excellent mechanical and electrical properties, such as over 20,000 cycles durability, transparency, flexibility, and power density up to 1.33 $W \cdot m^{-2}$. The device has a linearity of up to 0.949 in the tensile range of 200% and 0.992 in the bending angle range from 30° to 90°, respectively. Through processing and encoding the electrical signals collected by multiple channels in independent or synergistic mode, a self-powered medical nursing HMI system attached to patient fingers was developed to provide real-time help and assistance for both patients and medical staff, which the demand for distress calls can be successfully transmitted with just gently bending fingers in diagnosis. This work exhibits the application value of the self-powered triboelectric sensor to the medical HMI field, and can be extended to other aspects, showing a broad impact in brain computer interface.

1. Introduction

With the growth of the aging population in the world, medical healthy monitoring has posed great challenges to the economic structure of society and the scarcity of medical staff and resources [1–3]. Therein, the human-machine interface plays the role of a bridge between medical nursing and digital virtual worlds [4–9]. One of the foundations of the human-machine interface is flexible, wearable, and self-powered sensors with multiple functions [10], which identify the physiological responses or movements of the human body and transform them into electronic signals for transmission, such as strain [11], pressure [12], vibration [13], and humidity [14]. These sensors can provide accurate instantaneous information feedback, but they are difficult to simultaneously be flexible, stretchable, and quick-response. Triboelectric nanogenerator (TENG), as an emerging technology of self-powered sensing which combines triboelectrification and electrostatic induction, possesses great application potential in promising next-generation flexible and stretchable electronic devices [15–20]. The TENG translates physical signals into electrical signals and may be utilized as a self-powered sensor without any external power supply, which is a promising solution to meet the challenges of prolonging the continuous running time of monitoring sensors [21–24]. The electrode materials for flexible-stretchable TENGs face the limitation of simultaneously having excellent tensile properties, sensitive response, biocompatibility, and

☆ Prof. Zhong Lin Wang, an author on this paper, is the Editor-in-Chief of Nano Energy, but he had no involvement in the peer review process used to assess this work submitted to Nano Energy. This paper was assessed, and the corresponding peer review managed by Professor Chenguo Hu, also an Associate Editor in Nano Energy.

* Corresponding author at: Beijing Institute of Nanoenergy and Nanosystems, Chinese Academy of Sciences, Beijing 101400, PR China.
E-mail addresses: jiangtao@binn.cas.cn (T. Jiang), chenbaodong@binn.cas.cn (B. Chen).
[1] These authors contributed equally to this work.
[2] **ORCID**: 0000–0002-4647–0089

https://doi.org/10.1016/j.nanoen.2022.107199
Received 23 February 2022; Received in revised form 13 March 2022; Accepted 25 March 2022
Available online 29 March 2022

transparency [25]. Therefore, it is critical to investigate and develop high performance flexible-stretchable conductive electrode materials for TENGs.

Traditional flexible conductive materials, such as carbon nanotubes, graphene, carbon paste, and silver nanowires or polymers doped with these conductive materials, are hardly allowed to be flexible and transparent electrode materials [26–30]. Compared with traditional conductive materials, hydrogels are emerging flexible electrode materials attributed to their excellent stretchability, conductivity, simple preparation process, and cost-effectiveness [31–33]. Meanwhile, Ionic hydrogels are good ionic conductors that can absorb and store a certain amount of water through chemical or physical cross-linking, and have quick diffusion properties and good mechanical properties [34–36]. However, their practical applications are highly restricted due to their

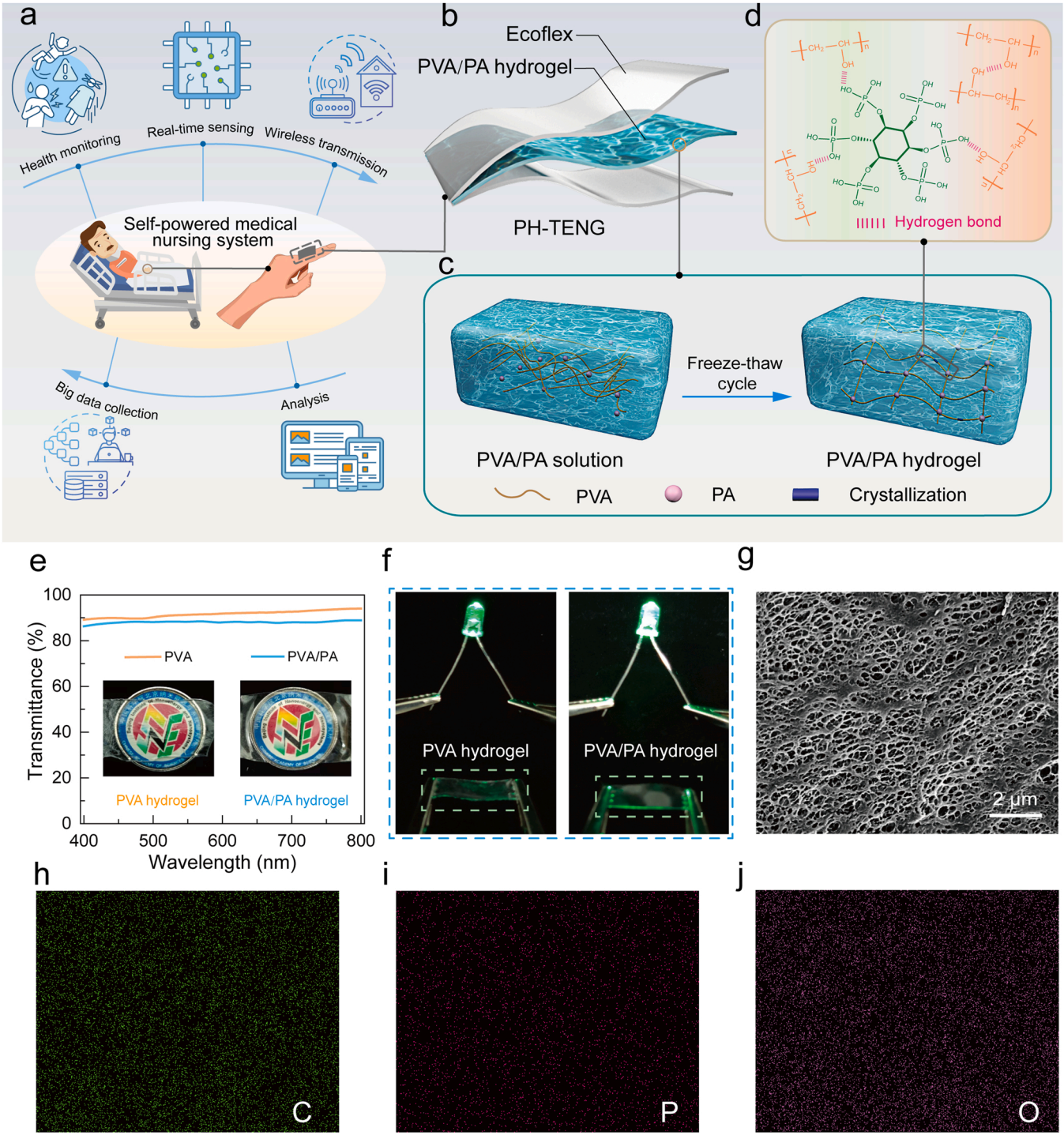

Fig. 1. Application and architecture of the PH-TENG and microstructure of the PVA/PA hydrogel. (a) Overview of PH-TENG assembled on the finger for health monitoring. (b) A schematic structure of the PH-TENG. (c) The schematic diagram of the PVA/PA hydrogel cross-linking process. (d) Schematic illustration of the as-synthesized PVA/PA hydrogel showing the cross-linking networks. (e) UV−vis spectra of the PVA hydrogel and PVA/PA hydrogel. (f) Intuitive comparison photographs of the electrical conductivity of PVA hydrogel and PVA/PA hydrogel. (g) SEM images of cross-section of PVA/PA hydrogel. (h-j) EDS mapping of PVA/PA hydrogel.

inability to combine the benefits of excellent conductivity [37,38], high transparency [39], strong mechanical strength [40,41], and fast response to external stimuli at the same time [42,43]. Phytic acid (PA) is an organic strong acid that can ionize a large number of freely moving hydrogen ions in water and contains a large number of hydroxyl that can form a large number of hydrogen bonds with polyvinyl alcohol (PVA). Therefore, an introduction of PA into PVA hydrogel may not only enhance mechanical properties and the conductivity of hydrogels but also provide the hydrogels with new performances to realize flexible-stretchable PVA/PA hydrogel materials.

In this work, we report a simple and effective process for fabricating a PVA/PA hydrogel-based triboelectric nanogenerator (PH-TENG) with excellent transparency, flexibility, stretchability, and electrical properties. With an effective contact area of 6 cm^2, the PH-TENG is capable of outputting a power density of 1.33 $W{\cdot}m^{-2}$ under an external load resistance of 500 MΩ. Owing to its excellent sensing linearity, the PH-TENG can be integrated into any joint of the body as an active self-powered flexible-stretchable triboelectric sensor. Through processing and encoding the electrical signals collected by multiple channels in independent or synergistic mode, a multichannel self-powered medical nursing HMI system attached to patient fingers was developed to provide real-time respondent and assistance for both patients and medical staff, which the demand for distress calls can be successfully transmitted with just gently bending fingers in diagnosis. Meanwhile, the PH-TENG can also be used as an energy collector to effectively harvest mechanical energy derived from ubiquitous mechanical motions. This work demonstrates great application foreground of the self-powered triboelectric sensor to the medical HMI field.

2. Results and discussion

The PH-TENG as a self-powered sensor for medical nursing has great potential application value, which possesses merits such as sensitive response, excellent mechanical properties, cost-effective, and large-scale production. Fig. 1a shows a conceptual schematic illustration of the PH-TENG was integrated into the finger joint as a self-powered flexible triboelectric sensor to deliver information, enabling real-time remote intelligent medical nursing management. Fig. 1b shows that PH-TENG with a sandwich structure is a typically single-electrode-mode. In addition, the Ecoflex is not only a superior sealing material for preventing water loss of the hydrogel, but also a high-performance triboelectric material, and was used to encapsulate the PVA/PA hydrogel as an electrode. After the PVA/PA hydrogel was attached with an external conductive copper wire, a single-electrode-mode PH-TENG was fabricated (Fig. S1, Supporting Information). The freeze-thaw cycle is a common method for the preparation of PVA hydrogels, since the crystallization of PVA and phase separation leading to gelation occur during this process [44,45]. Therefore, the PVA/PA hydrogel was prepared by the one-step freeze-thaw method, as shown in Fig. 1c. The PVA polymer chains are randomly arranged and distributed in the aqueous solution, and the physical cross-linker PA was randomly distributed among the PVA chains, forming mixed PVA/PA solution after stirring at 90 ℃ for 2 h. By a freeze-thaw cycle, the mixed solution is transformed into a flexible-stretchable and transparent PVA/PA hydrogel (Fig. S2a-e, Supporting Information). In the same preparation method without PA, pure PVA hydrogel was prepared and used as a comparison sample. The detailed preparation processes of the hydrogels and PH-TENG can be seen in the experimental section and Fig. S3 (Supporting Information). Fig. 1d shows that phytic acid, which contains abundant hydroxyl groups, can physically cross-linking with the hydroxyl groups on PVA to produce a large number of hydrogen bonds, greatly improving the mechanical strength of hydrogels. At the same time, a small number of hydrogen bonds can also be formed between PVA.

Compared with the pure PVA hydrogel with a transmittance of 94%, the PVA/PA hydrogel with a transmittance of 89% still has good optical transparency (Fig. 1e). These two hydrogels were placed on the top of an icon that acts as a background, and the image on the icon can be seen clearly (the inset of Fig. 1e). When the PVA hydrogel and PVA/PA hydrogel are linked to LED light circuits, respectively, it is evident that the LED in the PVA/PA hydrogel circuit is brighter (Fig. 1f), which due to the large number of hydrogen ions ionized from PA in the PVA/PA hydrogel. Fig. 1g shows that the PVA/PA hydrogel has a highly cross-linked dense microporous network structure at the cross-section, whereas pure PVA hydrogel has larger pores across the cross-section (Fig. S4, Supporting Information). The EDS mapping images of C, P, and O elements can be seen in Fig. 1h-j, demonstrating that PVA and PA are uniformly distributed in the PAV/PA hydrogel. Thus, the dense microporous network structure provides a continuous conduction path for ion transport [46].

The mechanical properties of conductive hydrogels are the most essential consideration for their application as stretched material. Therefore, the mechanical characteristics of PVA/PA hydrogels doped with various mass fractions of PA are compared. With the increase of PA mass fraction, the stress-strain of PVA/PA hydrogels improved obviously, followed by a significant drop (Fig. 2a). Detailed naming of PVA/PA_X hydrogels containing different mass fractions of PA can be found in the experimental section. The PVA/PA_{30} hydrogel can achieve a tensile strength of up to 550% at a peak strength of 1.7 MPa with an optimal PA mass fraction of 30%. To further investigate the stability of PVA/PA_{30} hydrogel, the hydrogel was tested in loading-unloading studies under various tensile circumstances at a stretching rate of 80 $mm{\cdot}min^{-1}$. Fig. 2b shows that the hysteresis is negligible before the 150% strain and a small hysteresis loop occurs when the strain reaches 200% and then the stretched hydrogel quickly recovers to its original state, which demonstrates that the synthesized hydrogel has excellent self-recovery performance following elongation. The stress-strain curves of the PVA/PA hydrogel essentially correspond with the loading-unloading cycles of 10 consecutive stretches of 150%, suggesting that the hydrogel has no noticeable softening during continuous loading-unloading and exhibits obvious fatigue resistance and stability (Fig. 2c). The stress-strain curve for stretching the hydrogel to 150% basically overlaps with the curve for unloading recovery (the inset of Fig. 2c), which means that the stretched hydrogel can revert to its original condition. The PVA/PA hydrogels with outstanding mechanical strength, toughness, and self-repair capacity may be due to the dense microporous network structure formed by hydrogen bonding between PVA and PA [47].

To further study the hydrogen bond between PVA and PA, the PVA/PA hydrogel was characterized by the Fourier transform infrared (FTIR) and the powder X-ray diffraction (XRD). As shown in Fig. 2d, the FTIR spectra of the pure PVA and PVA/PA hydrogel show typical stretching vibration peaks at 3270 cm^{-1} that are attributed to hydroxyl groups. The characterized peaks of hydroxyl groups at 3270 cm^{-1} become wider as the mass fraction of PA increases, probably due to the large number of hydroxyl groups involved in the formation of hydrogen bonds during physical cross-linking. The XRD pattern of the PVA hydrogel presented prominent peaks corresponding to the (101), (102) planes, and then the characteristic peaks gradually faded with the increase of the mass fraction of PA, indicating the influence on the crystallinity of PVA by changing the PA content (Fig. 2e). The water content of hydrogel is one of the key parameters to maintain good mechanical and electrical characteristics. After being exposed to air for eight hours, the water content of the hydrogel remained at 40% (Fig. S5, Supporting Information). As a strong organic acid, PA can fully ionize in water-rich hydrogels to generate a huge number of free hydrogen ions that can migrate directionally under a given voltage, giving PVA/PA hydrogels significant electrical conductivity without the need for any conductive materials. As a result, the conductivity of PVA-PA hydrogel may be strongly influenced by the PA content, that is, the higher PA concentration corresponding to improved electrical conductivity. Fig. 2f indicates that the conductivity of the PVA/PA hydrogel improves dramatically when compared to pure PVA hydrogel, reaching 7.2 S/m at a mass fraction of PA of 30%, and then it increases slowly after a larger

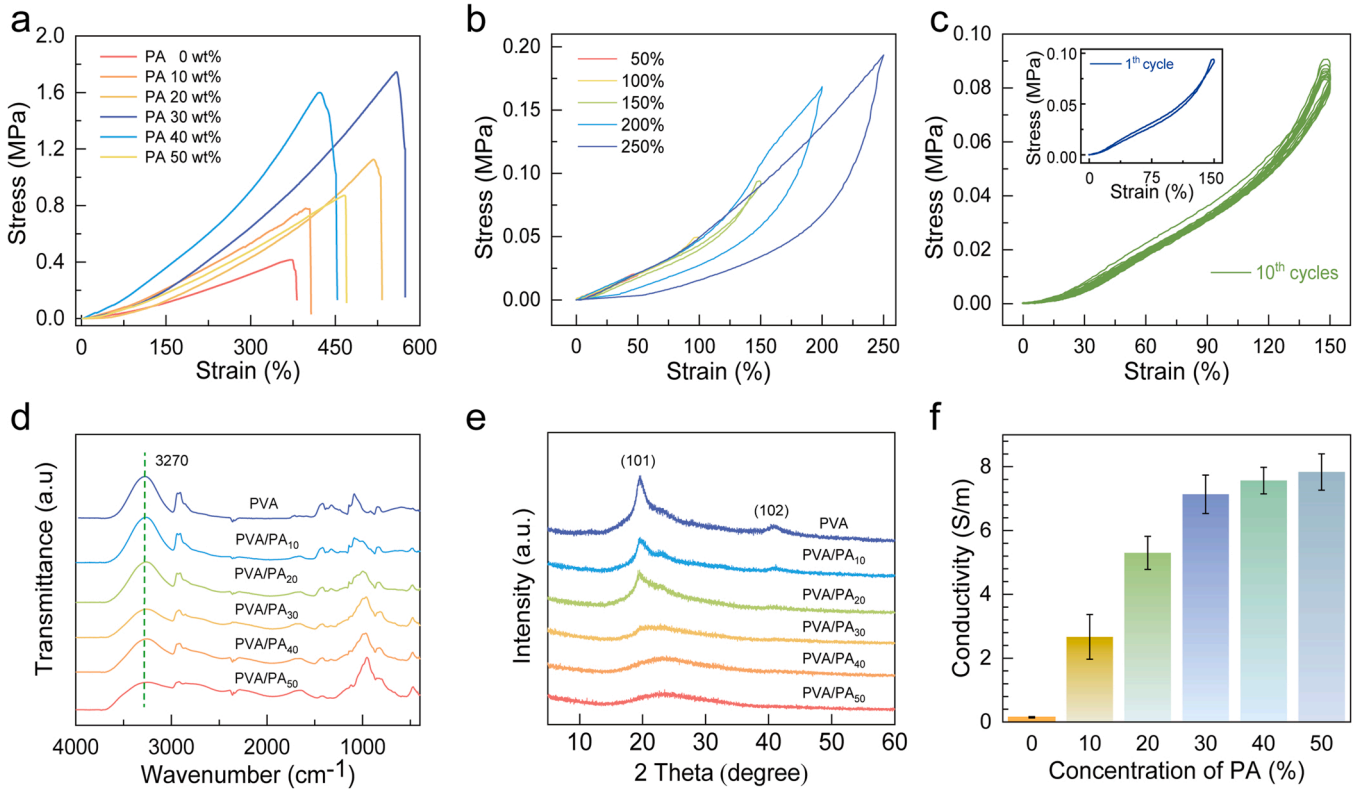

Fig. 2. Mechanical properties and spectroscopic characterization of hydrogels. (a) Stress-strain curve of PVA/PA hydrogels containing different mass fractions of PA. (b) Stress-strain curve of PVA/PA hydrogel under the consecutive loading-unloading tests under different strains. (c) Stress-strain curve of PVA/PA hydrogel for ten unloading-loading tests at a 150% strain, where the inset shows the stress-strain curve under an unloading-loading test. (d) FTIR spectra and (e) XRD patterns of PVA/PA hydrogels containing different mass fractions of PA. (f) Conductivity of PVA/PA hydrogels containing different mass fractions of PA.

mass fraction of PA. Meanwhile, we can utilize a 0.26 mm thick PVA/PA hydrogel to raise up the 500 g weight (Fig. S6a, b, Supporting Information).

Based on the excellent performance of the PVA/PA hydrogel, we sealed the enhanced hydrogels with Ecoflex silicone rubber (Fig. S1, Supporting Information). Due to the tight and optimized sealing process, the PH-TENG was placed in the air at room temperature for 7 days and its weight remaining was up to 99.7%, (Fig. S7, Supporting Information), demonstrating the silicone rubber effectively prevents the PVA/PA hydrogel from losing water. The PH-TENG exhibits excellent flexibility that allows it to tolerate arbitrary deformations without any mechanical damage, such as bending, contorting, and stretching more than 300% of its original length (Fig. S8a-d, Supporting Information). The stress-strain curve of Teng shows that it can return to its original state after 300% tension (Fig. S8e). Here, the PH-TENG utilizes PVA/PA hydrogel as an electrode to enable ion transportation for electrostatic screening of triboelectric charges in the Ecoflex, as shown in Fig. 3a. At the initial state (Fig. 3a, i), surface charges are induced on the two materials according to the triboelectric effect when a Latex film is completely contacted with the Ecoflex of the PH-TENG under an external mechanical force, with the same amount of positive and negative triboelectric charges distributed at the Latex and silicone rubber surfaces, respectively. When the Latex is gradually moving away from the Ecoflex of the PH-TENG, the static charges at the surface of the rubber will cause the hydrogen ions within the PVA/PA hydrogel to migrate to balance the static charges, generating a layer of excessive ions at the interface of PVA/PA hydrogel (Fig. 3a, ii). Meanwhile, the electrical double layer developed at the interfaces of copper wire and PVA/PA hydrogel will be polarized, resulting in the formation of the same number of charges with opposing polarity at the hydrogel-copper wire contact. To produce the double layer, electrons flow from the copper wire to the ground through external circuits at the same time. Next, with the Latex moving far enough, the circuit no longer generates charge movement due to negative charges on the Ecoflex being completely screened by the positive ions in the PVA/PA hydrogel (Fig. 3a, iii). Finally, when the Latex is approaching back to the Ecoflex, the whole process is reversed, and an electron flux in the opposite direction is transferred from the ground to the hydrogel-copper wire interface through the external load (Fig. 3a, iv). When the contact-separation motion between the Latex and Ecoflex is repeated, the alternative current will be formed continuously. During an external force cycle including contacting and separating, the current signal output by PH-TENG under short-circuit conditions verifies the mechanism mentioned above (Fig. 3b).

Based on the flexible and stretchable properties, we manufactured PH-TENG based on PVA/PA_{30} hydrogel as an electrode to systematically measure the electrical output performance. Since the output of the PH-TENG is greatly affected by the dielectric material, the impact of several common dielectric materials on the electrical output of the single-electrode mode PH-TENG is initially investigated, and Latex is found to be the best dielectric material for the output of PH-TENG (Fig. S9a-c, Supporting Information). As a result, Latex was utilized as a dielectric substance in later experiments. When a doping concentration of PA is 30%, the PH-TENG produced the output performance with the open-circuit voltage (V_{OC}) of 197 V, the short-circuit current (I_{SC}) of 1.8 μA, and the charge transfer amount (Q_{SC}) of 67 nC, which was promoted four times compared with the undoped PA (Fig. S9d-f, Supporting Information). The electrical output performance of the PH-TENG under various frequencies was measured. With the increase of frequency, the open-circuit voltage and the charge transfer amount remain relatively consistent at 201 V and 67 nC, respectively, and the short-circuit current increases linearly to 3.4 μA at 4 Hz (Fig. 3c-e). In addition, as a self-powered flexible-stretchable sensor, it is crucial for the PH-TENG to produce a stable signal output under different stretching. Fig. 3f-h

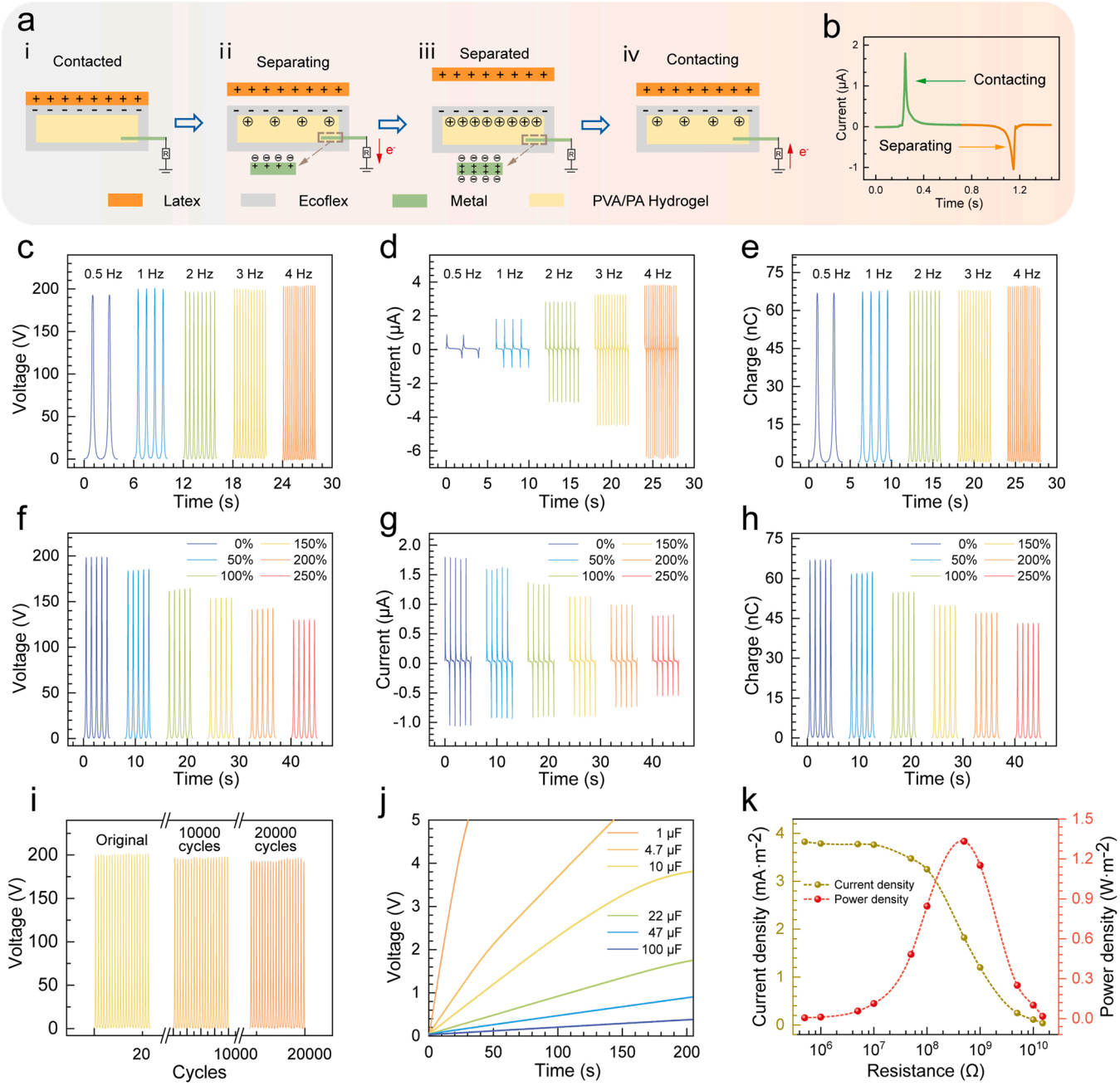

Fig. 3. The working principles and output performance of the PH-TENG. (a) A schematic working principle of the single-electrode mode PH-TENG. (b) The output signal of the PH-TENG under short-circuit conditions and once external force circulation. (c) Open-circuit voltage, (d) short-circuit current, and (e) transferred charge amount of the PH-TENG under different working frequencies. (f) Open-circuit voltage, (g) short-circuit current, and (h) transferred charge amount of the PH-TENG at different stretches. (i) Durability of the PH-TENG device when testing for various cycles. (j) The charging voltage curves of different capacitors by the PH-TENG. (k) Variation of the output current density and power density with the external loading resistance.

illustrates the output characteristics of the PH-TENG under different stretched. Under the tensile strain state of 250%, the electrical output can still be maintained at a high level, the open-circuit voltage, the short-circuit current, and the charge transfer amount reaches 130 V, 1.8 μA, and 43 nC, respectively. Notably, the electrical output decreases with the increase in the stretching length, which might be attributed to the smaller contact area between Latex and Ecoflex during the stretching process. The output stability of the PH-TENG was tested at a frequency of 1 Hz on a linear motor under 20,000 contact-separation continuous cycles, and the voltage remains constant, demonstrating that the PH-TENG has outstanding durability and potential application value (Fig. 3i). It was also found that the output of the PH-TENG decreased only slightly after seven days of testing (Fig. S7, Supporting Information). The charging capability of the PH-TENG was investigated by charging different capacitors, exhibiting fast charging capability (Fig. 3j). From the load output characteristics in Fig. 3k, the output power density can be calculated as following equation: $P=I_{SC}^2R/S$, where R and S are resistance and the upper surface area of PH-TENG, respectively, which shows a maximum output power density of 1.33 $W{\cdot}m^{-2}$ with the load resistance of 500 MΩ.

The PH-TENG can generate large electrical signals by a lateral stretch due to the porous structure of the PVA/PA hydrogel as transport channels for a large number of hydrogen ions increasing the electrification performance. Two clamps were used to fixed the two ends of the PH-

TENG and then installed on a linear motor and a 3D displacement platform for tensile testing (Fig. S10a, Supporting Information). Fig. 4a shows that the open-circuit voltage is increased linearly with the increase of stretching length of the PH-TENG. When the PH-TENG was stretched to 200% of the initial length, it generated 5.3 V, 2.5 nA, and 0.56 nC in open-circuit voltage, short-circuit current, and transferred charge, respectively. (Fig. S10b-d, Supporting Information). During the stretching process, the longer the stretching is, the smaller the corresponding transport channels are compressed, and the more positively charged water in the transport channel would be squeezed out of the transport channels, which will create a large potential difference and attract more external charges to balance the potential difference. The electrical output of the PH-TENG increases with the increase of the stretch length, which may attribute to water containing hydrogen ions in the transport channel would be squeezed out to the surface of the Ecoflex. Another possible reason is that the distance of the gap between the hydrogel and Ecoflex decreases as the PH-TENG was stretched.

Based on the proportional relationship between the open-circuit voltage and the corresponding stretch length of the PH-TENG, the PH-TENG can be utilized as a body motion monitoring sensor benefited from the real-time and fast response. We used tape to fix the two ends of the PH-TENG to the experimenter's finger, wrist, elbow, and knee. Fig. 4b shows that PH-TENG can convert bending angles of 30°, 45°, 60°, 75°, and 90° into voltage signals, which increase linearly with the increase of finger bending angle. The voltage signal of the PH-TENG at each angle of the cycle bending is extremely stable, and the signal corresponding to different angles is clearly distinguished. Then, we have performed the two processes of the PH-TENG following the finger from straight to full bend and from straight to half bend, and the voltage signal corresponding to the two processes presented a double relationship, as shown in Fig. 4c. The PH-TENG is also fixed on the elbow to perform the same bending angle as the one fixed on the finger, resulting

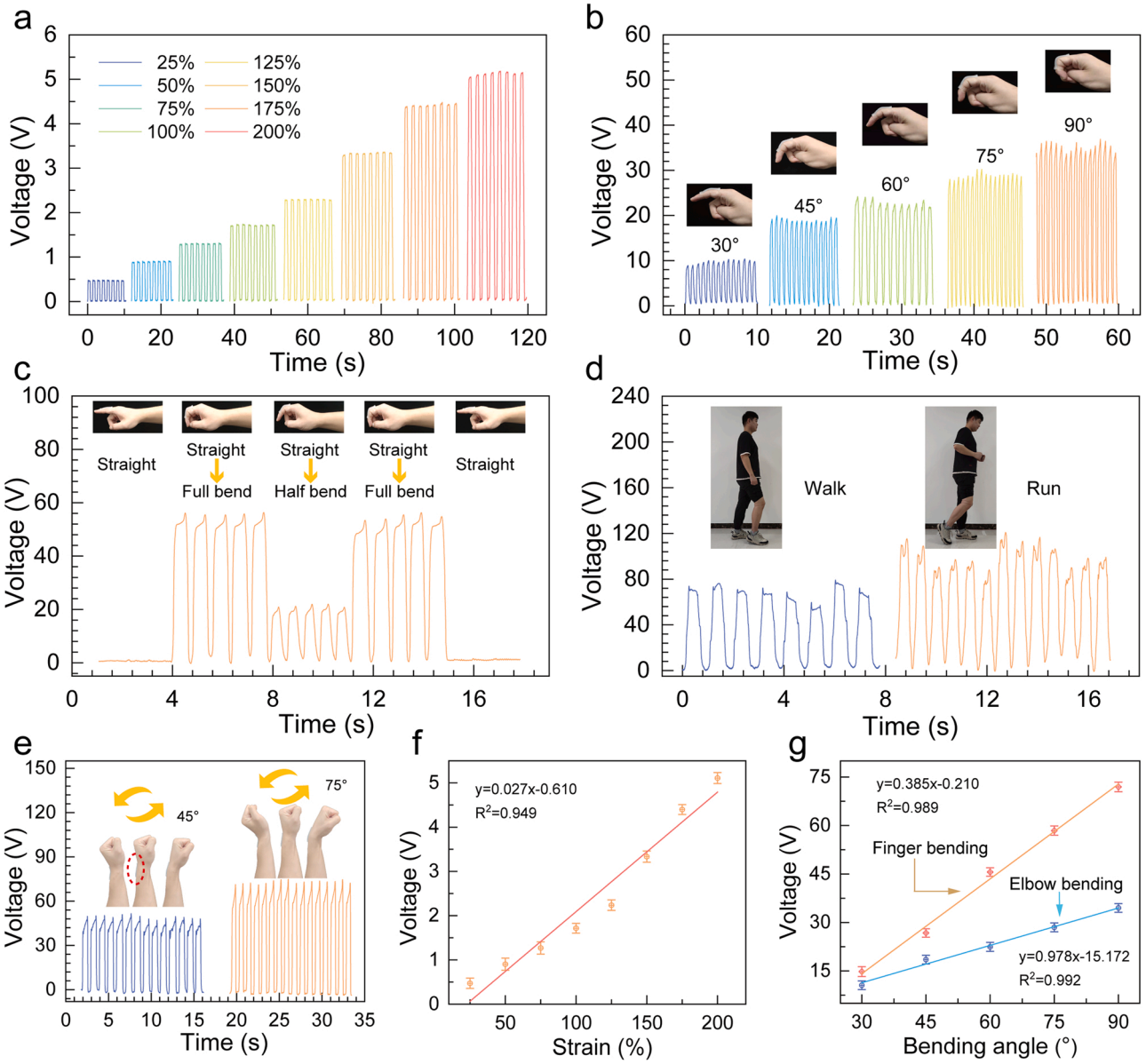

Fig. 4. Output voltages generated by different stretched states and self-powered sensors for monitoring joint bending degree. (a) The output voltage of PH-TENG under different strains. (b) Voltage signals in response to the finger bends in 30°, 45°, 60°, 75°, and 90°. (c) Voltage signals in response to finger bends. (d) Real-time voltage outputs demonstrate the different motion states of walking and running. (e) Detection of the wrist flexion by fixing a PH-TENG to the wrist. (f) The summarized relationship and linear fitting between output voltages and stretch length of PH-TENG. (g) The relationship between output voltages and bending angle of finger and elbows.

in a similar trend in which the voltage signal increases as the elbow bending angle increases (Fig. S11, Supporting Information). To further verify the reliability of PH-TENG for monitoring strenuous body movement, the PH-TENG is fixed on the experimenter's knee to monitor the voltage signal of walking and running, as shown in Fig. 4d. The peak voltage signal of the PH-TENG is somewhat higher in the running than in the walking state, and the waveform of motion monitoring in these two states is substantially different. When compared to walking, the voltage signal waveform of the running condition has a continuous small peak, which might be ascribed to the PH-TENG not to be consistent with knees bend and makes secondary contacts with the skin during a single bending cycle.

Fig. 4e shows that the output of the PH-TENG, which is fixed to the wrist and bent at 45° and 75°, increases as the wrist bending angle increases, but the waveform of the PH-TENG is completely different from that of the one fixed on the finger and elbow. What is more interesting, even though the actual stretched length by body bending was not enough 100%, the voltages generated by body bending were up to several tens of volts higher than those generated by stretching the PH-TENG to 200% of its original length, which is due to the two ends of the PH-TENG being firmly adhered by tape, but gaps between the central section and the skin. In the process of joint bending, the skin rubs against PH-TENG, and also the PH-TENG is stretched to a certain length. As the stretch rate of the PH-TENG increases, the output voltage shows a clear increasing trend. Fig. 4f shows good linearity ($R^2 = 0.949$) between the output voltage signal and the stretch rate of the PH-TENG. When the generator is fixed at the finger and elbow joints, the relationship between output voltage signals generated by bending the finger and elbow and the angle of bending are almost linear ($R^2 = 0.989$, 0.992) (Fig. 4g). The excellent linear relationship and stability indicate that the PH-TENG could be used as a sensitive and self-powered sensor for the applications of the self-powered daily and clinical body motion monitoring and messaging.

Nowadays, the medical monitoring system is facing the pressure of a serious shortage of medical staff and medical resources, so it is imperative to use intelligent management to improve work efficiency. Fig. 5a depicts prospective applications of the triboelectric sensor were integrated the fingers of the patient as a micro-sensor, which bends with the bending of the fingers to generate a signal transmitted to the guardians for help, realizing real-time monitoring and intelligent management in the medical monitoring system. The electrical signals generated by the synchronous movement of the triboelectric sensor and the hand joints are collected by a multi-channel data acquisition card, processed and displayed by the software based on LabVIEW. Here, for multi-channel output voltage measurements, synchronous data capture cards with integrated signal conditioning features are employed. The equivalent circuit of the measurement system is shown in Fig. S12 (Supporting Information). As shown in Fig. 5b, when five triboelectric sensors are fixed to the fingers and stretched with the bending of the fingers, a distinctive electrical signal will be produced. Then, the real-time voltage signals can be detected simultaneously by the front-end circuit and transmitted to the chip through the operational amplifier. Finally, the signals are wirelessly transmitted to the mobile phone or computer, and the real-time signals are analyzed based on LabVIEW and displayed on the interface of mobile phone or computer.

In the process of signal processing, 3 V is defined as the threshold voltage. When the output signal generated by the triboelectric sensor bending is greater than the threshold voltage of 3 V, it is recorded as "1", indicating that a voltage signal is collected. When the peak voltage is less than the threshold voltage, which is recorded as "0". Here, a 5-channel data acquisition card is used to collect the signal. The voltage signal can be collected by single channel or multi-channel combination, which can be converted into different letters, so any information can be conveyed using a mix of gestures. Fig. 5c depicts various letters corresponding to specific codes. Triboelectric sensors are fastened to the fingers of the experimenter and connected to a multi-channel data acquisition card to convey the needs of the experimenter. The electrical signals generated by triboelectric sensors are encoded by gray code and then processed into corresponding letters by a LabVIEW software (Fig. S13, Supporting Information). The real-time voltage signals of all the channels and the real-time needs of "hungry", "help", and "thirsty" for help seekers are controlled by different gesture combinations (Fig. 5d, and Fig. S14, Supporting Information).

Fig. 5e shows that triboelectric sensors are integrated into the fingers and connected with the multi-channel electrometer acquisition board. The interface of the self-powered medical nursing system displaying the real-time patient's help information and each signal corresponds to a specific letter. The enlarged real-time voltage signal waveform of the word ("hungry") is shown in Fig. 5f, containing a specific letter corresponding to each voltage signal, which illustrates the excellent performance of this system in processing the signal generated by the triboelectric sensor and coding of voltage peaks. To further verify the stability of the system, the messages of "help" and "thirsty" are conveyed by controlling gestures (Fig. 5g, h, and Fig. S15, Supporting Information). Detailed demonstration videos of the experimenter delivering "hungry", "help", and "thirsty" can be obtained from Video S1–3 (Supporting Information). It is worth noting that the letters generated by one channel control have only one voltage signal, and those with two channels control generate two voltage signals at the same moment (Fig. S16, Supporting Information). As a self-powered flexible triboelectric sensor, the PH-TENG with fast response, stable output, and safety shows great application prospects in medical nursing and postoperative rehabilitation. Meanwhile, 60 EDs were easily illumined by directly tapping the PH-TENG with Latex (Video S4, Supporting Information), revealing great application potentials of the PH-TENG in low-frequency mechanical energy harvesting.

3. Conclusion

In summary, we developed a transparent flexible-stretchable PH-TENG, which can be attached with any joints of the body as an active triboelectric sensor for self-powered sensing in HMI. Benefiting from simple and effective design strategy, the PH-TENG possesses excellent mechanical and electrical properties, such as over 20,000 cycles durability, good flexibility-stretchability, and power density of 1.33 $W \cdot m^{-2}$. The PH-TENG has a linearity of up to 0.949 in the tensile range of 200% and 0.992 in the bending angle range from 30° to 90°, respectively. To make the effectivity and promotion for clinician-patient communication, a multichannel self-powered medical nursing HMI system attached to patient fingers is developed to provide real-time respondent and assistance for both patients and medical staff. Through processing and encoding the electrical signals collected by multiple channels in independent or synergistic mode, the demand for distress calls can be successfully transmitted with just gently bending fingers in diagnosis, such as the nursing information of "hungry", "help", and "thirsty". This work is promising for being developed into an alternative strategy in medical nursing HMI field, and can be extended to other aspects, showing a broad impact in intelligent flexible electronics and brain computer interface.

4. Experimental section

4.1. Materials

Poly (vinyl alcohol) 1799 ($[—CH_2CHOH—]_n$, alcoholysis degree 98–99% (mol/mol^{-1}), molecule weight: 44.05) was purchased by Shanghai Aladdin Biochemical Technology Co., Ltd. Phytic acid ($C_6H_{18}O_{24}P_6$, molecule weight: 660.04, ≥ 70 wt% in water) were purchased from Sinopharm Chemical Reagent Co., Ltd. Ecoflex 00–30 silicone rubber (Mix ratio 1A:1B by volume or weight, Total Net Wt.: 0.90 kg) was purchased from Smooth-On company, USA. The deionized water was purified by Shanghai Hetai Edi-S10 ultrapure water machine

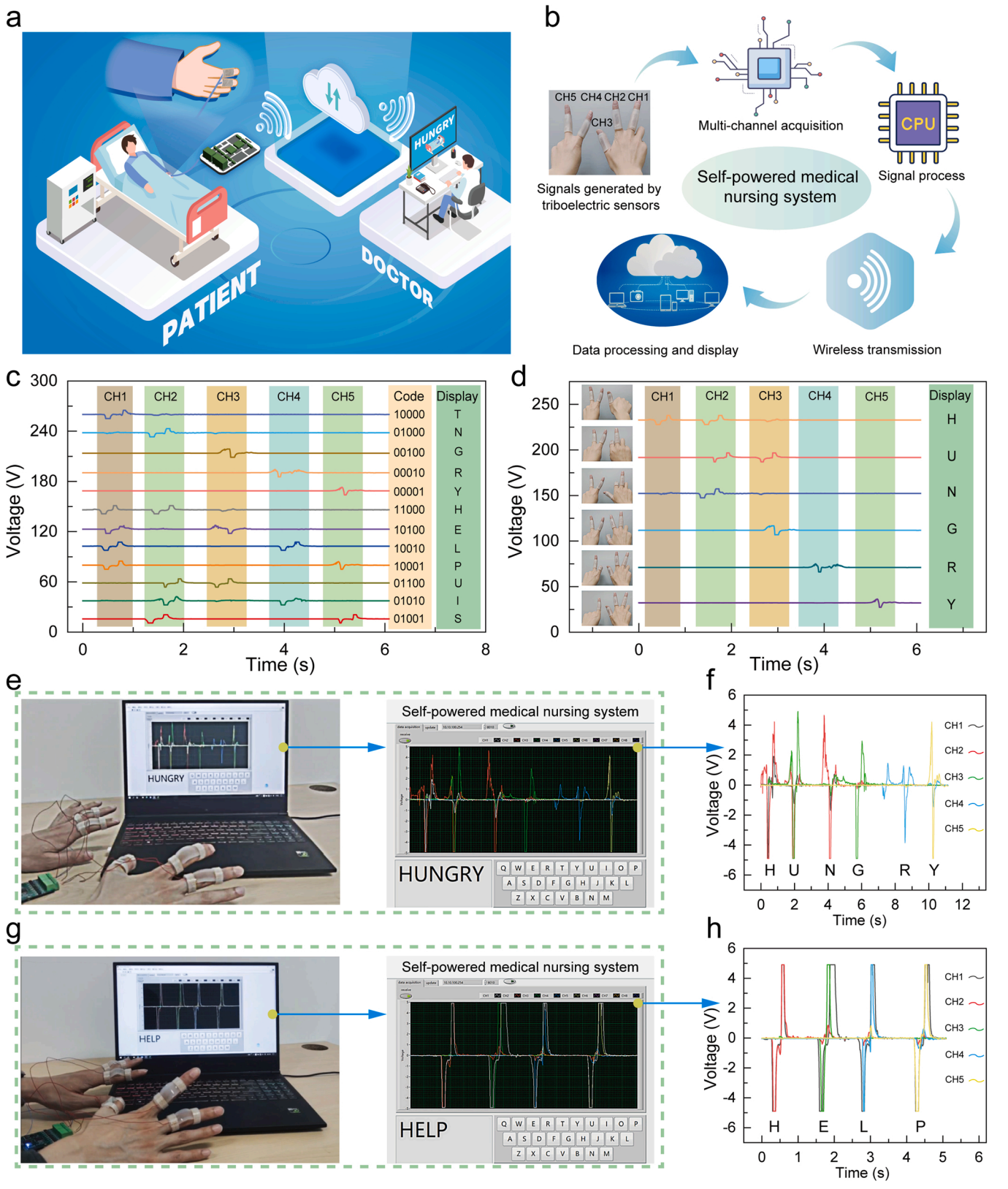

Fig. 5. Application of the PH-TENG in the medical nursing field for direct transmission of information. (a) Schematic illustration of a self-powered medical nursing system for remote monitoring and delivering the patient's help message. (b) Scheme diagram of the triboelectric sensor involved in the self-powered medical nursing system. (c) The signals collected by multiple channels are encoded by gray code and defined into corresponding letters (d) The combination of different gestures expresses the word hungry. (e) The scene graph of PH-TENGs being integrated into the fingers to transmit information and the interface of system real-time displays the patient's requirements. (f) Real-time voltage waveform from multi-channel data acquisition card. (g) The word "help" is displayed on the interface of the system and (h) an enlarged view of the corresponding voltage waveform.

in the laboratory.

4.2. Synthesis of PVA/PA hydrogel

PVA/PA hydrogel was synthesized by a physical-crosslinking method. PVA/PA hydrogels containing PA with different mass fractions were labeled as PVA/PA$_X$. First, PVA (1.36 g, 12 wt%) was dissolved to different masses of deionized water (10, 8.864, 7.728, 6.592, 5.456, and 4.320 g). Then, varied PA weights (0, 1.136, 2.272, 3.408, 4.544, and 5.680 g) were added to the above-mentioned corresponding blended solution, making the total mass of each mixture 11.36 g. At the same time, PVA/PA$_X$ homogeneous solutions with different mass fractions of PA were obtained by magnetic stirring at 90 ℃ for 2 h until all dissolved PVA powders have completely cross-linked with phytic acid. After the prepared PVA/PA$_X$ homogeneous solutions were cooled to room temperature, the six mixtures were poured into different molds and followed by a freeze-thaw cycle treatment of freezing at − 20 ℃ for 12 h and thawing at room temperature for 3 h, and hydrogels of PVA/PA$_0$ (PA content: 0 wt%), PVA/PA$_{10}$ (PA content: 10 wt%), PVA/PA$_{20}$, PVA/PA$_{30}$, PVA/PA$_{40}$, and PVA/PA$_{50}$ were finally achieved.

4.3. Fabrication of the PH-TENG

The PH-TENG was a sandwiched structure with Ecoflex as top and bottom layers and the PVA/PA hydrogel encapsulated inside the Ecoflex, whose detailed structure and size were depicted in Fig. S1 in the Supporting Information. Ecoflex 00–30 silicone rubber (mix ratio 1 A:1B by weight) was transferred to a prefabricated 2×4.5 cm^2 rectangular model, pumped with vacuum to remove air bubbles, and then kept it at room temperature for 2 h to obtain the bottom layer. Next, the prepared fix-sized PVA/PA$_X$ hydrogel was placed on the center of the bottom layer and attached a conductive copper foil as an external electrode. Then, the Ecoflex with the same quality as the bottom one was poured into the model and then performed the same vacuum, solidify processes as the bottom layer to fabricate the PH-TENG. The PVA/PA$_X$ hydrogel was completely sealed by Ecoflex 00–30 silicone rubber, which could effectively prevent the hydrogel from losing water, while ensuring the same displacement of the hydrogel and the silicone rubber when PH-TENG is stretched.

4.4. Characterization of materials and the PH-TENG

The FTIR spectra were obtained by a Fourier transform infrared spectrometer (Bruker, Vertex80V). The XRD patterns were measured with a powder XRD (PANalytical B. V., Xpert3 Power). The micro-topography of PVA/PA$_X$ hydrogel and EDS mapping were acquired using Navo field emission scanning electron microscope (FEI, Navo NanoSEM 450). The stress-strain test of the PVA/PA$_X$ hydrogel was performed by a YL-S71 Tensile testing machine at a stretching rate of 80 mm·min^{-1}. The UV–vis–NIR spectra were recorded with a Shimadzu UV-3600 spectrophotometer at room temperature. The conductivity measurement was performed on an electrochemical workstation (Metrohm PQSTAT302N). A linear motor (LinMot 1100) was used to provide the input of mechanical motions for research of the stretching of the PH-TENG. The open-circuit voltage, short-circuit current, and transferred charge amount were recorded by a Keithley 6514 electrometer.

CRediT authorship contribution statement

Jin Yang: Writing – original draft, Methodology. **Jie An:** Data curation, Validation. **Yanshuo Sun:** Investigation, Formal analysis. **Jianjun Zhang:** Visualization. **Lulu Zu:** Validation. **Hao Li:** Data curation. **Tao Jiang:** Methodology, Formal analysis, Supervision. **Baodong Chen:** Writing – review & editing, Supervision, Resources. **Zhong Lin Wang:** Conceptualization, Resources.

Declaration of Competing Interest

The authors declare that they have no known competing financial interests or personal relationships that could have appeared to influence the work reported in this paper.

Acknowledgements

J.Y. and J.A. contributed equally to this work. The authors acknowledge the support from Natural Science Foundation of Beijing Municipality (2192062), supported by the National Key R & D Project from Minister of Science and Technology (2021YFA1201601), National Natural Science Foundation of China (Grant No. 52192610).

Appendix A. Supporting information

Supplementary data associated with this article can be found in the online version at doi:10.1016/j.nanoen.2022.107199.

References

[1] Q. Tang, M.-H. Yeh, G. Liu, S. Li, J. Chen, Y. Bai, L. Feng, M. Lai, K.-C. Ho, H. Guo, C. Hu, Whirligig-inspired triboelectric nanogenerator with ultrahigh specific output as reliable portable instant power supply for personal health monitoring devices, Nano Energy 47 (2018) 74–80.
[2] F. Yi, Z. Zhang, Z. Kang, Q. Liao, Y. Zhang, Recent advances in triboelectric nanogenerator-based health monitoring, Adv. Funct. Mater. 29 (2019), 1808849.
[3] X. Zhao, H. Askari, J. Chen, Nanogenerators for smart cities in the era of 5G and internet of things, Joule 5 (2021) 1391–1431.
[4] J. Yang, Y. Sun, J. Zhang, B. Chen, Z.L. Wang, 3D-printed bearing structural triboelectric nanogenerator for intelligent vehicle monitoring, Cell Rep. Phys. Sci. 2 (2021), 100666.
[5] Y. Luo, Z. Wang, J. Wang, X. Xiao, Q. Li, W. Ding, H.Y. Fu, Triboelectric bending sensor based smart glove towards intuitive multi-dimensional human-machine interfaces, Nano Energy 89 (2021), 106330.
[6] G. Yao, L. Xu, X. Cheng, Y. Li, X. Huang, W. Guo, S. Liu, Z.L. Wang, H. Wu, Bioinspired triboelectric nanogenerators as self-powered electronic skin for robotic tactile sensing, Adv. Funct. Mater. 30 (2020), 1907312.
[7] Z. Lin, G. Zhang, X. Xiao, C. Au, Y. Zhou, C. Sun, Z. Zhou, R. Yan, E. Fan, S. Si, L. Weng, S. Mathur, J. Yang, J. Chen, A. Personalized, Acoustic interface for wearable human–machine interaction, Adv. Funct. Mater. 32 (2022), 2109430.
[8] Z. Zhou, K. Chen, X. Li, S. Zhang, Y. Wu, Y. Zhou, K. Meng, C. Sun, Q. He, W. Fan, E. Fan, Z. Lin, X. Tan, W. Deng, J. Yang, J. Chen, Sign-to-speech translation using machine-learning-assisted stretchable sensor arrays, Nat. Electron. 3 (2020) 571–578.
[9] J.H. Han, K.M. Bae, S.K. Hong, H. Park, J.-H. Kwak, H.S. Wang, D.J. Joe, J.H. Park, Y.H. Jung, S. Hur, C.D. Yoo, K.J. Lee, Machine learning-based self-powered acoustic sensor for speaker recognition, Nano Energy 53 (2018) 658–665.
[10] Z. Wu, T. Cheng, Z.L. Wang, Self-powered sensors and systems based on nanogenerators, Sensors 20 (2020) 2925.
[11] Y. Fan, Z. Shen, X. Zhou, Z. Dan, L. Zhou, W. Ren, T. Tang, S. Bao, C. Nan, Y. Shen, Highly sensitive strain sensor from topological-structure modulated dielectric elastic nanocomposites, Adv. Mater. Technol. 7 (2021), 2101190.
[12] M. Jian, K. Xia, Q. Wang, Z. Yin, H. Wang, C. Wang, H. Xie, M. Zhang, Y. Zhang, Flexible and highly sensitive pressure sensors based on bionic hierarchical structures, Adv. Funct. Mater. 27 (2017), 1606066.
[13] Q. He, Y. Wu, Z. Feng, C. Sun, W. Fan, Z. Zhou, K. Meng, E. Fan, J. Yang, Triboelectric vibration sensor for a human-machine interface built on ubiquitous surfaces, Nano Energy 59 (2019) 689–696.
[14] A.R. Mule, B. Dudem, S.A. Graham, J.S. Yu, Humidity sustained wearable pouch-type triboelectric nanogenerator for harvesting mechanical energy from human activities, Adv. Funct. Mater. 29 (2019), 1807779.
[15] Y. Liu, B. Chen, W. Li, L. Zu, W. Tang, Z.L. Wang, Bioinspired triboelectric soft robot driven by mechanical energy, Adv. Funct. Mater. 31 (2021), 2104770.
[16] C. Ning, K. Dong, R. Cheng, J. Yi, C. Ye, X. Peng, F. Sheng, Y. Jiang, Z.L. Wang, Flexible and stretchable fiber-shaped triboelectric nanogenerators for biomechanical monitoring and human-interactive sensing, Adv. Funct. Mater. 31 (2020), 2006679.
[17] J. Yi, K. Dong, S. Shen, Y. Jiang, X. Peng, C. Ye, Z.L. Wang, Fabric-based triboelectric nanogenerators as self-powered human-machine interactive keyboards, Nano-Micro Lett. 13 (2021) 103.

[18] S. Zhang, M. Bick, X. Xiao, G. Chen, A. Nashalian, Leveraging triboelectric nanogenerators for bioengineering, J. Chen, Matter 4 (2021) 845–887.
[19] G. Chen, Y. Li, M. Bick, J. Chen, Smart textiles for electricity generation, Chem. Rev. 120 (2020) 3668–3720.
[20] B.Y. Lee, D.H. Kim, J. Park, K.I. Park, K.J. Lee, C.K. Jeong, Modulation of surface physics and chemistry in triboelectric energy harvesting technologies, Sci. Technol. Adv. Mater. 20 (2019) 758–773.
[21] J. An, P. Chen, Z. Wang, A. Berbille, H. Pang, Y. Jiang, T. Jiang, Z.L. Wang, Biomimetic hairy whiskers for robotic skin tactility, Adv. Mater. 33 (2021), e2101891.
[22] J. Luo, Z. Wang, L. Xu, A.C. Wang, K. Han, T. Jiang, Q. Lai, Y. Bai, W. Tang, F. R. Fan, Z.L. Wang, Flexible and durable wood-based triboelectric nanogenerators for self-powered sensing in athletic big data analytics, Nat. Commun. 10 (2019) 5147.
[23] Y. Zou, J. Xu, Y. Fang, X. Zhao, Y. Zhou, J. Chen, A hand-driven portable triboelectric nanogenerator using whirligig spinning dynamics, Nano Energy 83 (2021), 105845.
[24] X. Gao, F. Xing, F. Guo, Y. Yang, Y. Hao, J. Chen, B. Chen, Z.L. Wang, A turbine disk-type triboelectric nanogenerator for wind energy harvesting and self-powered wildfire pre-warning, Mater. Today Energy 22 (2021), 100867.
[25] X. Luo, L. Zhu, Y.C. Wang, J. Li, J. Nie, Z.L. Wang, A flexible multifunctional triboelectric nanogenerator based on MXene/PVA hydrogel, Adv. Funct. Mater. 31 (2021), 2104928.
[26] X. Chen, Y. Song, H. Chen, J. Zhang, H. Zhang, An ultrathin stretchable triboelectric nanogenerator with coplanar electrode for energy harvesting and gesture sensing, J. Mater. Chem. A 5 (2017) 12361–12368.
[27] R.-C. Wang, Y.-C. Lin, P.-T. Chen, H.-C. Chen, W.-T. Chiu, Anomalous output performance enhancement of RGO-based triboelectric nanogenerators by Cu-bonding, Nano Energy 86 (2021), 106126.
[28] M. He, W. Du, Y. Feng, S. Li, W. Wang, X. Zhang, A. Yu, L. Wan, J. Zhai, Flexible and stretchable triboelectric nanogenerator fabric for biomechanical energy harvesting and self-powered dual-mode human motion monitoring, Nano Energy 86 (2021), 106058.
[29] G. Jian, Q. Meng, Y. Jiao, L. Feng, H. Shao, F. Wang, F. Meng, Hybrid PDMS-TiO2-stainless steel textiles for triboelectric nanogenerators, Chem. Eng. J. 417 (2021), 127974.
[30] G.-H. Lim, S.S. Kwak, N. Kwon, T. Kim, H. Kim, S.M. Kim, S.-W. Kim, B. Lim, Fully stretchable and highly durable triboelectric nanogenerators based on gold-nanosheet electrodes for self-powered human-motion detection, Nano Energy 42 (2017) 300–306.
[31] Y. Long, Y. Chen, Y. Liu, G. Chen, W. Guo, X. Kang, X. Pu, W. Hu, Z.L. Wang, A flexible triboelectric nanogenerator based on a super-stretchable and self-healable hydrogel as the electrode, Nanoscale 12 (2020) 12753–12759.
[32] F. Sheng, J. Yi, S. Shen, R. Cheng, C. Ning, L. Ma, X. Peng, W. Deng, K. Dong, Z. L. Wang, Self-powered smart arm training band sensor based on extremely stretchable hydrogel conductors, ACS Appl. Mater. Interfaces 13 (2021) 44868–44877.
[33] P. Zhang, Y. Chen, Z. Guo, W. Guo, X. Pu, Z.L. Wang, Stretchable, transparent, and thermally stable triboelectric nanogenerators based on solvent-free ion-conducting elastomer electrodes, Adv. Funct. Mater. 30 (2020), 1909252.
[34] M.C. Arno, M. Inam, A.C. Weems, Z. Li, A.L.A. Binch, C.I. Platt, S.M. Richardson, J. A. Hoyland, A.P. Dove, R.K. O'Reilly, Exploiting the role of nanoparticle shape in enhancing hydrogel adhesive and mechanical properties, Nat. Commun. 11 (2020) 1420.
[35] H. Sun, Y. Zhao, C. Wang, K. Zhou, C. Yan, G. Zheng, J. Huang, K. Dai, C. Liu, C. Shen, Ultra-Stretchable, durable and conductive hydrogel with hybrid double network as high performance strain sensor and stretchable triboelectric nanogenerator, Nano Energy 76 (2020), 105035.
[36] T. Zhu, C. Jiang, M. Wang, C. Zhu, N. Zhao, J. Xu, Skin-inspired double-hydrophobic-coating encapsulated hydrogels with enhanced water retention capacity, Adv. Funct. Mater. 31 (2021), 2102433.
[37] X. Jing, H. Li, H.Y. Mi, P.Y. Feng, X. Tao, Y. Liu, C. Liu, C. Shen, Enhancing the performance of a stretchable and transparent triboelectric nanogenerator by optimizing the hydrogel ionic electrode property, ACS Appl. Mater. Interfaces 12 (2020) 23474–23483.
[38] C.J. Lee, H. Wu, Y. Hu, M. Young, H. Wang, D. Lynch, F. Xu, H. Cong, G. Cheng, Ionic conductivity of polyelectrolyte hydrogels, ACS Appl. Mater. Interfaces 10 (2018) 5845–5852.
[39] C. Zhang, Y. Zhou, H. Han, H. Zheng, W. Xu, Z. Wang, Dopamine-triggered hydrogels with high transparency, self-adhesion, and thermoresponse as skinlike sensors, ACS Nano 15 (2021) 1785–1794.
[40] G. Li, J. Zhang, F. Huang, S. Wu, C.-H. Wang, S. Peng, Transparent, stretchable and high-performance triboelectric nanogenerator based on dehydration-free ionically conductive solid polymer electrode, Nano Energy 88 (2021), 106289.
[41] P. Jiang, P. Lin, C. Yang, H. Qin, X. Wang, F. Zhou, 3D Printing of dual-physical cross-linking hydrogel with ultrahigh strength and toughness, Chem. Mater. 32 (2020) 9983–9995.
[42] M. Li, X. Wang, B. Dong, M. Sitti, In-air fast response and high speed jumping and rolling of a light-driven hydrogel actuator, Nat. Commun. 11 (2020) 3988.
[43] Y. Hu, M. Zhang, C. Qin, X. Qian, L. Zhang, J. Zhou, A. Lu, Transparent, conductive cellulose hydrogel for flexible sensor and triboelectric nanogenerator at subzero temperature, Carbohydr. Polym. 265 (2021), 118078.
[44] Y. Guo, K. Zheng, P. Wan, A flexible stretchable hydrogel electrolyte for healable all-in-one configured supercapacitors, Small 14 (2018), e1704497.
[45] W. Li, H. Lu, N. Zhang, M. Ma, Enhancing the properties of conductive polymer hydrogels by freeze-thaw cycles for high-performance flexible supercapacitors, ACS Appl. Mater. Interfaces 9 (2017) 20142–20149.
[46] L. Shao, Y. Li, Z. Ma, Y. Bai, J. Wang, P. Zeng, P. Gong, F. Shi, Z. Ji, Y. Qiao, R. Xu, J. Xu, G. Zhang, C. Wang, J. Ma, Highly sensitive strain sensor based on a stretchable and conductive Poly(vinyl alcohol)/Phytic Acid/NH2-POSS hydrogel with a 3D microporous structure, ACS Appl. Mater. Interfaces 12 (2020) 26496–26508.
[47] Y. Wang, X. Zhang, Y. Song, Y. Zhao, L. Chen, F. Su, L. Li, Z.L. Wu, Q. Zheng, Ultrastiff and tough supramolecular hydrogels with a dense and robust hydrogen bond network, Chem. Mater. 31 (2019) 1430–1440.

Jin Yang received his B.S. degree from Anqing Normal University in 2019. He is currently a Master candidate student at Guangxi University and a joint student in Beijing Institute of Nanoenergy and Nanosystems, Chinese Academy of Sciences. His research interests are mainly focused on self-powered sensing systems and wearable/flexible electronic device based on triboelectric nanogenerator.

Jie An received his B.S. degree in Maritime Engineering from Dalian Maritime University in 2017. Now he is pursuing his Ph. D. degree in Beijing Institute of Nanoenergy and Nanosystems, Chinese Academy of Sciences. His research interests are mainly focused on clean energy harvesting and self-powered sensor systems based on triboelectric nanogenerator.

Yanshuo Sun received her B.S. degree from Zaozhuang University in 2019. She is currently a Master candidate student at Guangxi University and a joint student in Beijing Institute of Nanoenergy and Nanosystems, Chinese Academy of Sciences. Her research interests are mainly focused on alternating current electroluminescence and wearable/flexible electronic device based on triboelectric nanogenerator.

Jianjun Zhang received his B.S. degree in Material Chemistry (2015) from TaiShan University and M.S. degree in MaterialsPhysics and Chemistry (2018) from Guizhou University. He is currently pursuing the Ph.D degree in Center on Nanoenergy Research in Guangxi University. He mainly focuses on the research of fabrication of triboelectric nanogenerators and nano devices.

Lulu Zu received her bachelor's degree at Henan University of Science and Technology in 2019. Now she is pursuing her Ph.D. degree in Beijing Institute of Nanoenergy and Nanosystems, Chinese Academy of Sciences. Her research interests are focused on wearable/flexible electronics and 3D-printed triboelectric nanogenerators.

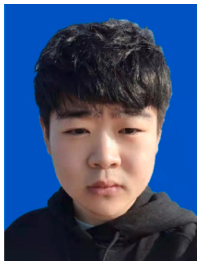

Hao Li is currently a Master candidate student at Guangxi University and a joint student in Professor Zhonglin Wang's group at Beijing Institute of Nanoenergy and Nanosystems, Chinese Academy of Sciences. His research interest focuses on triboelectric nanogenerator for energy harvesting.

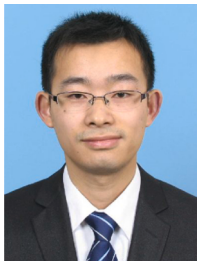

Dr. Tao Jiang is a professor in the Beijing Institute of Nanoenergy and Nanosystems, Chinese Academy of Sciences. He received his B.S. and Ph.D. degrees from School of Materials Science and Engineering, in 2008 and 2014, respectively, from East China University of Science and Technology. After graduation, he worked in the Beijing Institute of Nanoenergy and Nanosystems as a postdoctoral research fellow. His research interests are the theoretical studies of triboelectric nanogenerators, and practical applications in blue energy harvesting.

Dr. Baodong Chen is an associate professor in Beijing Institute of Nanoenergy and Nanosystems (BINN), Chinese Academy of Sciences (CAS); School of Nanoscience and Technology, University of Chinese Academy of Sciences. He received his PhD degree from School of Materials Science and Engineering in 2015, from Inner Mongolia University of Technology, China. Prior to joining the faculty at BINN in 2018, he was a postdoctoral fellow at National Center for Nanoscience and Technology. His research interests include nanocomposite materials, nanogenerator, self-powered sensing systems, and 2D and 3D printed flexible electronics.

Prof. Zhong Lin Wang received his Ph.D. degree from Arizona State University in physics. He now is the Hightower Chair in Materials Science and Engineering, Regents' Professor at Georgia Tech, the chief scientist and director of the Beijing Institute of Nanoenergy and Nanosystems, Chinese Academy of Sciences. Prof. Wang has made original and innovative contributions to the synthesis, discovery, characterization and understanding of fundamental physical properties of oxide nanobelts and nanowires, as well as applications of nanowires in energy sciences, electronics, optoelectronics and biological science. His discovery and breakthroughs in developing nanogenerators establish the principle and technological road map for harvesting mechanical energy from environmental and biological systems for powering personal electronics. His research on self-powered nanosystems has inspired the worldwide efforts in academia and industry for studying energy for micro-nano-systems, which is now a distinct disciplinary in energy research and future sensor networks. He coined and pioneered the fields of piezotronics and piezophototronics by introducing piezoelectric potential gated charge transport process in fabricating new electronic and optoelectronic devices.